10-2004

Photometric Identification of Cool White Dwarfs

M. Kilic
University of Texas at Austin

D. E. Winget
University of Texas at Austin, dew@astro.as.utexas.edu

Ted von Hippel
Embry-Riddle Aeronautical University, vonhippt@erau.edu

C. F. Claver
Kitt Peak National Observatory, National Optical Observatory, cclaver@noao.edu

The Astronomical Journal, 128:1825–1833, 2004 October

PHOTOMETRIC IDENTIFICATION OF COOL WHITE DWARFS[1]

M. Kilic,[2,3] D. E. Winget, and Ted von Hippel
Department of Astronomy, University of Texas at Austin, 1 University Station C1400, Austin, TX 78712; kilic@astro.as.utexas.edu, dew@astro.as.utexas.edu, ted@astro.as.utexas.edu

and

C. F. Claver[4]
Kitt Peak National Observatory, National Optical Astronomy Observatory, P.O. Box 26732, Tucson, AZ 85726; cclaver@noao.edu
Received 2004 April 14; accepted 2004 June 17

ABSTRACT

We investigate the use of a narrowband DDO51 filter for photometric identification of cool white dwarfs. We report photometric observations of 30 known cool white dwarfs with temperatures ranging from 10,000 K down to very cool temperatures ($\leq$3500 K). Follow-up spectroscopic observations of a sample of objects selected using this filter and our photometric observations show that DDO51 filter photometry can help select cool white dwarf candidates for follow-up multiobject spectroscopy by rejecting 65% of main-sequence stars with the same broadband colors as the cool white dwarfs. This technique is not selective enough to efficiently feed single-object spectrographs. We present the white dwarf cooling sequence using this filter. Our observations show that very cool white dwarfs form a sequence in the $r - \mathrm{DDO}$ versus $r - z$ color-color diagram and demonstrate that significant improvements are needed in white dwarf model atmospheres.

Key words: stars: evolution — white dwarfs

Online material: color figures

1. INTRODUCTION

White dwarf stars, remnants of the earliest and all subsequent generations of star formation, are tracers of the age and evolution of the Galaxy. They are initially hot and consequently cool rapidly, although the cooling rate slows as their temperature drops, allowing the oldest white dwarfs to remain visible. Because the cooling rate slows, any census finds more and more white dwarfs at lower and lower temperatures (and luminosities) until, quite abruptly, we find no more of them. Such a census is called the white dwarf luminosity function. Attempts to exploit the white dwarfs as chronometers showed that the white dwarf luminosity function was a map of the history of star formation in the disk and that there was a shortfall of low-luminosity white dwarfs—the inevitable consequence of the finite age of the disk (Liebert 1979; Winget et al. 1987; Liebert et al. 1988).

The cool end of the white dwarf luminosity function was estimated from 43 objects found in the Luyten Half Second Proper Motion Survey (Luyten 1979; Liebert et al. 1988). Proper-motion surveys are the most common method of searching for white dwarfs. Since the white dwarfs are intrinsically faint, they must be close to be seen; therefore, they tend to have higher proper motions than most other stars with similar magnitudes. Proper-motion surveys cannot detect white dwarfs with small tangential velocities, however. Therefore, they have complicated and hard-to-quantify completeness problems. Wood & Oswalt (1998) argue that the ages inferred from the Liebert et al. (1988) white dwarf luminosity function must be considered uncertain by 15% from sampling statistics alone. More importantly, depending on how the data are binned, as many as three or as few as one of the 43 objects occupy the last bin in the white dwarf luminosity function, precisely the point where all of the age leverage resides. A recent sample of white dwarfs in wide binaries (Oswalt et al. 1996) shows a somewhat lower luminosity downturn, which, at the 2 σ level, is consistent with no downturn at all in the coolest bin. The simple fact is the fainter age-dependent end of the white dwarf luminosity function is not yet satisfactorily constrained by observation or theory.

An investigation of the cool end of the white dwarf luminosity function that is focused on disentangling theoretical uncertainties in the cooling process would greatly benefit from a much larger kinematically unbiased sample of cool white dwarfs. The details of the constituent input physics can affect the implied ages of white dwarfs below $\log(L/L_{\odot}) \sim -4.2$ by as much as 2–3 Gyr and hence are critical for using white dwarfs as chronometers (Hawkins & Hambly 1999; Montgomery et al. 1999; Salaris et al. 2000).

A magnitude-limited, kinematically unbiased sample of white dwarfs can be obtained through a photometric survey. A unique color signature is necessary to photometrically identify a white dwarf among the many other field stars. The magnitude limit of a survey is also a critical factor in the search for cool white dwarfs; if the survey cannot provide sufficiently high signal-to-noise ratio data for $M_V \sim 16$, it cannot recognize cool low-luminosity white dwarfs. Broadband photometric surveys can be used to find hot white dwarfs because of their blue colors. Recently, Kleinman et al. (2004) found 2551

[1] Based on observations obtained with the Hobby-Eberly Telescope, which is a joint project of the University of Texas at Austin, Pennsylvania State University, Stanford University, Ludwig-Maximilians-Universität München, and Georg-August-Universität Göttingen.

[2] Visiting Astronomer, Kitt Peak National Observatory, National Optical Astronomy Observatory (NOAO), which is operated by the Association of Universities for Research in Astronomy (AURA), Inc., under cooperative agreement with the National Science Foundation (NSF).

[3] Visiting Astronomer, Cerro Tololo Inter-American Observatory, NOAO, which is operated by AURA, Inc., under cooperative agreement with NSF.

[4] Kitt Peak National Observatory, NOAO, which is operated by AURA, Inc., under cooperative agreement with NSF.

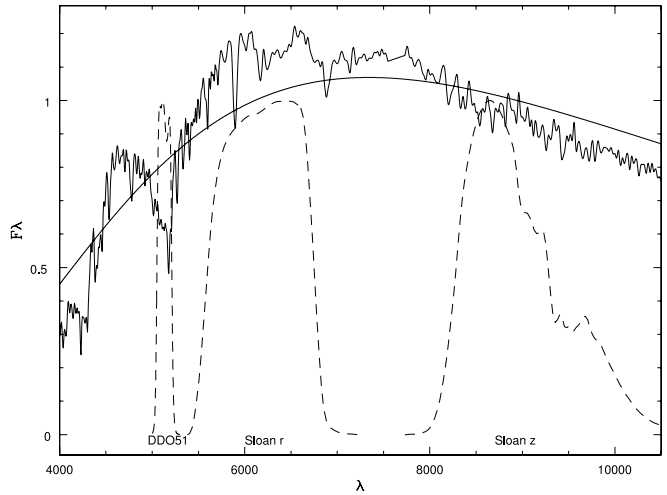

FIG. 1.—Template spectra for a K5 V star (Pickles 1998) and a 5000 K blackbody. The tracing for the DDO51, *r*, and *z* filters are shown as dashed lines. The greatest difference between the blackbody and the template stellar spectra, Mg absorption, is apparent in this figure.

new white dwarfs with $T_{\rm eff} \geq 8000$ K in the Sloan Digital Sky Survey (SDSS) Data Release 1. Unfortunately, the broadband colors of cool white dwarfs are identical to the metal-poor subdwarfs. The lack of discovery of cool white dwarfs in the SDSS emphasizes the fact that cool white dwarfs are indistinguishable from subdwarfs and main-sequence stars in broadband photometric observations (e.g., Claver 1995).

In this paper, we investigate the use of the narrowband DDO51 filter for photometric identification of cool white dwarfs. We present imaging data and follow-up spectroscopy of nine cool white dwarf candidates in § 2. In § 3, our observations of 30 known cool white dwarfs including four ultracool white dwarfs are discussed. We also show the cooling sequence for these white dwarfs. We discuss the efficiency and possible use of this filter for photometric identification of cool white dwarfs in § 4, along with the observed blue turnoff of very cool white dwarfs.

2. FORWARD APPROACH: PHOTOMETRY TO SPECTROSCOPY

Broadband filter photometry has a limited capacity to distinguish metal-poor subdwarfs from cool white dwarfs. In the absence of significant line blanketing, both the white dwarfs and subdwarfs have broadband colors that closely approximate those of a blackbody. However, by comparing the flux through a magnesium absorption line–centered filter, e.g., DDO51, several authors have suggested that cool white dwarfs could be distinguished from other field stars of similar $T_{\rm eff}$ (Claver 1995; Harris et al. 2001; Kilic et al. 2003). This is because the majority of cool white dwarfs have essentially featureless spectra around 5150 Å, where subdwarfs and main-sequence stars show significant absorption from the Mg *b* triplet and/or MgH. Figure 1 shows a template spectra for a K5 V star (Pickles 1998) and a 5000 K blackbody spectrum along with the tracing of the DDO51, *r*, and *z* filters. It is clear from this figure that white dwarfs should be distinguishable from the subdwarf stars using the narrowband DDO51 filter and a combination of broadband filters. We note that relative to a blackbody, the K-star spectrum deviates both above and below the blackbody line—depending on the wavelength sampled. Thus, the color indices could just as well be affected by features in the K star beyond 5150 Å as at that wavelength. However, Mg absorption is the strongest feature in the range sampled by the chosen filters, *r*, *z*, and DDO51.

To test the above claim, E. Olsewzki kindly provided us with DDO51 photometry of an area of 2 deg^2 from the Spaghetti Survey (Morrison et al. 2000), which overlaps with the SDSS fields. A color-color diagram for this field is shown in Figure 2. Two hot white dwarfs found by the SDSS are shown as open circles. Spectroscopically identified QSOs and stars (which are not white dwarfs) are shown as open squares and filled triangles, respectively. Spectral identifications and photometric data for these objects are given in Table 1. A typical error bar for these objects is shown in the bottom left corner of the figure. White dwarfs are expected to be separated from main-sequence stars in this color-color diagram (see Fig. 4.11 of Claver 1995); we have selected stars that deviate from the main sequence as possible cool white dwarf candidates. Cool white dwarf candidates selected for follow-up spectroscopy at the 9.2 m Hobby-Eberly Telescope (HET) and the McDonald 2.7 m Harlan-Smith Telescope are shown as filled circles (see Table 2 for photometric information).

2.1. *Observations*

Follow-up spectroscopy of nine white dwarf candidates in the Spaghetti Survey field was obtained in 2002 April and May using the HET and in 2003 February using the 2.7 m Harlan-Smith Telescope. We used the HET equipped with the Marcario Low Resolution Spectrograph (LRS) to obtain low-resolution spectroscopy of four cool white dwarf candidates. Grism 1 with a 2″ slit produced spectra with a resolution of 16 Å over the range 4000–10000 Å. Spectroscopy for four additional stars was obtained at the McDonald 2.7 m Telescope with the Imaging Grism Instrument (IGI) and TK4 camera using the holographic grating, which produced spectra with a resolution of 12 Å over the range 4000–8000 Å. A spectrophotometric standard star was observed each night for flux calibration. Ne-Cd calibration lamp exposures were taken after each observation with the HET, and Ne-Ar lamp calibrations were taken at the beginning of the night for the 2.7 m observations. The data were reduced using standard IRAF[5] routines.

2.2. *Results*

The observed spectra for selected white dwarf candidates from the HET and the 2.7 m and the fitted template spectra are shown as thin lines in Figures 3*a* and 3*b*, respectively. Spectra are ordered by $g - r$ color. We have used Pickles (1998) template spectra to classify the observed spectra qualitatively. The object numbers, coordinates, and the assigned spectral classifications are shown on the bottom right corner of the figures. Two of the objects observed at the HET, SDSS J114149.41−001140.4 and SDSS J120709.16−011247.2, show blue excesses. SDSS J114149.41−001140.4 also shows strong Hβ and Hγ lines. Therefore, we classify these stars as white dwarf+late-type star spectroscopic binaries. Figures 3*a* and 3*b* show that none of the observed white dwarf candidates are actually single white dwarfs. This discovery contradicted the expected yield of the DDO51 filter, which led us to reconsider our strategy for using this filter. We then

[5] IRAF is distributed by NOAO, which is operated by AURA, Inc., under cooperative agreement with NSF.

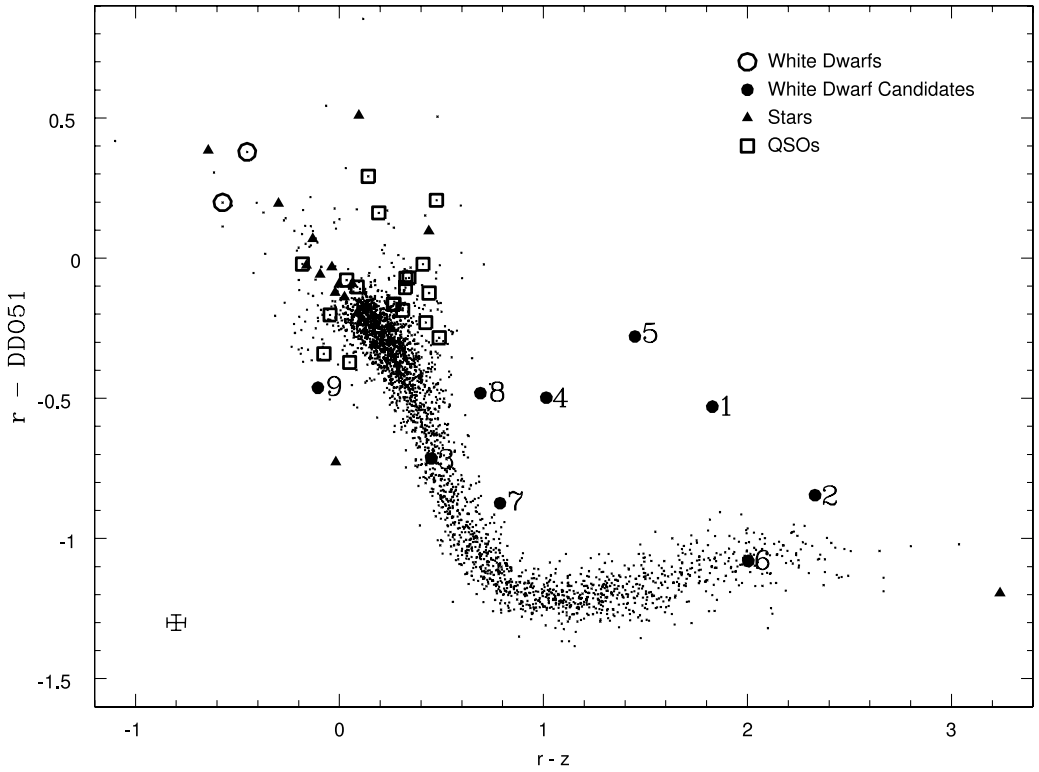

FIG. 2.—An $r - \mathrm{DDO51}$ vs. $r - z$ color-color diagram of a 2 deg^2 field from the Spaghetti Survey, which overlaps with the Sloan Digital Sky Survey fields. Two hot, spectroscopically identified white dwarfs are shown as open circles. Quasars and stars (which are not white dwarfs) are shown as open squares and filled triangles, respectively. Cool white dwarf candidates selected for follow-up spectroscopy are shown as filled circles. We note that objects 3 and 6 were not selected as cool white dwarf candidates, but they happened to be positioned on the slit during our observations of cool white dwarf candidates.

pursued a reverse approach, which is described in the next section.

3. REVERSE APPROACH: SPECTROSCOPY TO PHOTOMETRY

Follow-up spectroscopy of photometrically selected cool white dwarf candidates resulted in the discovery of subdwarf stars and unusual binaries instead of cool white dwarfs. To test the effectiveness of the filter in distinguishing cool white dwarfs from subdwarf stars, we decided to observe known cool white dwarfs with the DDO51 filter.

3.1. *Observations and Results*

DDO51, *r*-, and *z*-band photometry of 30 known cool white dwarfs with temperatures ranging from 10,000 K down to very cool temperatures ($T_{\rm eff} \leq 3500$ K) was obtained at the CTIO 4 m Blanco Telescope and Kitt Peak 4 m Mayall Telescope equipped with the $8\mathrm{k} \times 8\mathrm{k}$ MOSAIC Imager in 2002 November and 2003 June, respectively. The MOSAIC Imager, when used with these 4 m telescopes, provides a $35' \times 35'$ field of view. The CCD images were processed with the standard procedures in the MSCRED package in IRAF v2.12. We adopted the reduction procedures used by the NOAO Deep Wide-Field Survey Team.[6] Images were bias-subtracted and flat-fielded using dome flats and sky flats. The *z*-band images were corrected for fringing using the fringing templates derived from the sky flats. We matched star positions in the fields with positions from the USNO-A V2.0 Catalog (Monet et al. 1998) to obtain a plate solution for each CCD. The rms differences between observed source positions and the USNO-A V2.0 Catalog were less than 0.″4. Using the derived astrometric solutions, images were projected to the same uniform (linear, 0.″258 pixel^{-1}) scale.

Source identifications were performed on the projected images using the SExtractor package (v2.1.6; Bertin & Arnouts 1996). The main motivation for using the SExtractor package was its morphological classification. SExtractor uses a neural network to classify objects as stars (stellarity=1) or galaxies (stellarity=0). Stellarity is a continuous variable that can take any value from 0 to 1. A comparison of stellarity indices with magnitudes show that objects with stellarity index $\geq$0.8 have reliable classification as stars. We tested the SExtractor and the IRAF routines WPHOT and PHOT to perform photometry on our images. WPHOT with a Gaussian weighting scheme gave the best results for fainter objects, and we therefore adopted WPHOT photometry. We selected all objects with a stellarity index larger than 0.8 and with photometric errors less than 0.1 mag for our analysis. Only those objects detected in each filter that matched up to within 0.″5 or better in each coordinate are included in our final catalogs.

Most of our observations were obtained under photometric conditions. Since we are mainly interested in the differential photometry between white dwarfs and the rest of the field stars, data from nonphotometric nights are also useful. We have cross-correlated color-color diagrams for each field with the data from the Spaghetti Survey and matched the observed field-star sequences to remove any photometric offsets from nonphotometric observing conditions. Figure 4 shows the

[6] MOSAIC reduction procedures can be found at http://www.noao.edu/noao/noaodeep/ReductionOpt/frames.html.

TABLE 1
OBJECTS WITH SDSS SPECTROSCOPY

Object	Plate MJD Fiber	DDO	u	g	r	i	z	σ_{DDO}	σ_u	σ_g	σ_r	σ_i	σ_z	Type
SDSS J101748.90−003124.5	271 51883 166	18.68	19.30	18.86	18.84	18.85	18.65	0.01	0.03	0.01	0.01	0.01	0.03	QSO
SDSS J101807.04−002003.3	271 51883 174	20.14	20.99	19.98	19.91	19.97	19.49	0.02	0.12	0.02	0.03	0.04	0.08	QSO
SDSS J101741.70−002934.1	271 51883 181	16.34	16.56	16.28	16.72	16.88	17.17	0.01	0.01	0.01	0.01	0.01	0.02	WD
SDSS J101651.74−003347.0	271 51883 226	19.14	18.93	19.01	18.95	18.65	18.64	0.01	0.02	0.02	0.01	0.01	0.04	QSO
SDSS J105907.68+010303.5	277 51908 361	19.26	19.20	19.17	18.88	18.78	18.83	0.01	0.03	0.01	0.02	0.02	0.04	QSO
SDSS J105934.61+011112.1	277 51908 377	17.81	18.82	17.86	17.50	17.38	17.34	0.01	0.02	0.01	0.03	0.01	0.02	Star
SDSS J110015.66+010740.5	277 51908 414	18.80	19.09	18.74	18.99	19.30	19.57	0.01	0.02	0.01	0.02	0.03	0.08	WD
SDSS J110010.68+010328.3	277 51908 416	16.89	18.97	17.63	17.40	17.31	17.30	0.01	0.02	0.01	0.02	0.02	0.02	Star
SDSS J112941.64+000545.3	281 51614 117	18.60	19.63	18.61	18.57	18.53	18.61	0.01	0.04	0.02	0.02	0.03	0.06	Star
SDSS J112837.56−000112.6	281 51614 142	19.05	19.57	18.35	18.32	18.38	18.34	0.01	0.03	0.01	0.01	0.01	0.03	Star
SDSS J112839.72+002644.3	281 51614 485	18.11	19.35	18.19	17.98	17.99	18.01	0.01	0.04	0.03	0.01	0.02	0.03	Star
SDSS J113015.48+002843.9	281 51614 551	17.74	17.71	17.68	17.72	17.93	17.90	0.01	0.01	0.02	0.02	0.02	0.02	QSO
SDSS J113026.84+002649.1	282 51658 348	20.20	20.01	19.99	20.09	19.83	19.77	0.02	0.05	0.03	0.03	0.04	0.11	QSO
SDSS J113031.57+002033.4	282 51658 353	17.95	18.08	18.04	17.87	17.88	17.84	0.01	0.01	0.02	0.01	0.02	0.02	QSO
SDSS J113003.26+000332.4	282 51658 356	19.63	19.64	19.53	19.55	19.37	19.23	0.01	0.04	0.02	0.03	0.04	0.09	QSO
SDSS J113009.77+001737.6	282 51658 357	19.70	20.89	19.81	19.80	19.40	19.36	0.02	0.06	0.03	0.03	0.02	0.06	Star
SDSS J114311.23−002133.0	283 51959 224	18.99	18.88	18.92	18.83	18.72	18.56	0.01	0.02	0.02	0.02	0.03	0.04	QSO
SDSS J114321.76−002941.5	283 51959 229	18.81	19.32	19.10	19.11	19.26	18.96	0.01	0.03	0.01	0.02	0.02	0.04	QSO
SDSS J114318.48−002254.9	283 51959 237	18.59	19.57	18.63	18.45	18.46	18.42	0.01	0.03	0.02	0.02	0.03	0.03	Star
SDSS J114210.47−002013.0	283 51959 238	19.08	19.36	19.16	18.89	18.87	18.76	0.01	0.03	0.02	0.03	0.05	0.04	QSO
SDSS J114137.14−002729.8	283 51959 262	18.61	18.94	18.75	18.59	18.42	18.18	0.01	0.02	0.01	0.02	0.01	0.03	QSO
SDSS J114151.31−000729.7	283 51959 398	17.10	18.05	17.17	16.90	16.82	16.81	0.01	0.01	0.01	0.01	0.02	0.02	Star
SDSS J114259.30−000156.5	283 51959 435	19.47	19.96	19.50	19.18	18.93	18.69	0.02	0.04	0.01	0.02	0.02	0.03	QSO
SDSS J120637.75−011246.6	286 51999 81	17.29	18.24	17.34	17.12	17.00	16.98	0.01	0.02	0.01	0.02	0.01	0.02	Star
SDSS J120631.48−010801.8	286 51999 85	19.37	20.38	19.44	19.12	19.02	18.87	0.01	0.07	0.02	0.02	0.03	0.06	Star
SDSS J120708.35−010002.5	286 51999 86	19.07	19.12	19.09	18.94	18.59	18.50	0.01	0.03	0.02	0.01	0.02	0.03	QSO
SDSS J123056.59−005306.4	289 51990 17	18.89	19.26	18.87	18.73	18.72	18.46	0.01	0.03	0.02	0.01	0.01	0.03	QSO
SDSS J123213.28−003106.3	289 51990 25	19.08	20.22	19.07	19.15	19.21	19.28	0.02	0.04	0.02	0.01	0.02	0.05	Star
SDSS J123051.62−004437.1	290 51941 284	18.00	19.00	17.84	17.97	18.03	18.14	0.01	0.02	0.02	0.02	0.02	0.03	Star
SDSS J123149.22−005550.4	290 51941 292	17.49	18.45	17.46	17.43	17.48	17.53	0.01	0.01	0.02	0.01	0.01	0.01	Star
SDSS J123140.81−004435.1	290 51941 293	18.71	19.68	18.75	18.62	18.58	18.56	0.01	0.03	0.02	0.02	0.02	0.04	Star
SDSS J123027.54−003633.3	290 51941 319	16.88	17.84	16.79	17.07	17.29	17.37	0.01	0.01	0.02	0.01	0.02	0.01	Star
SDSS J131941.10−004340.6	296 51984 184	20.46	23.35	20.85	19.27	17.21	16.03	0.03	0.68	0.04	0.02	0.01	0.01	Star
SDSS J131938.76−004940.0	296 51984 189	17.59	17.73	17.54	17.48	17.50	17.40	0.01	0.02	0.02	0.01	0.01	0.02	QSO
SDSS J143143.80−005011.4	306 51637 129	18.05	18.31	18.09	17.85	17.81	17.89	0.01	0.02	0.02	0.02	0.02	0.02	QSO
SDSS J143158.36−004303.9	306 51637 138	19.14	19.06	18.99	18.80	18.74	18.88	0.01	0.02	0.03	0.02	0.02	0.03	QSO
SDSS J143153.06−002824.3	306 51637 194	17.82	17.29	17.66	18.21	18.91	18.85	0.01	0.02	0.02	0.02	0.03	0.04	SDO
SDSS J143037.11−004748.9	306 51637 255	16.98	17.92	17.02	16.89	16.88	16.89	0.01	0.02	0.01	0.01	0.02	0.01	Star
SDSS J145321.76+010130.6	538 52029 212	19.95	20.53	20.10	20.15	19.96	19.68	0.02	0.06	0.02	0.03	0.04	0.08	QSO
SDSS J145244.19+010954.9	538 52029 251	19.97	20.21	20.21	19.90	19.88	19.56	0.02	0.05	0.03	0.03	0.03	0.08	QSO

color-color diagram for 30 known white dwarfs and surrounding field stars. Field stars from the Spaghetti Survey and our study are shown as black dots. A typical error bar for the field stars is shown in the bottom left corner of the figure. A good match between our data and the Spaghetti Survey data is apparent in this figure. Known white dwarfs are shown as filled circles. Our synthetic photometry of white dwarf model atmospheres (Saumon & Jacobson 1999; D. Saumon 2004, private communication) for pure H (*solid line*) and pure He (*dashed line*) white dwarfs with 7000 K $\gtrsim T_{\rm eff} \gtrsim$ 3000 K and a blackbody (*dotted line*) are also shown. Dashed-dotted lines represent mixed H/He atmospheres for 3500 and 3000 K white dwarfs with different compositions ($\log [N({\rm He})/N({\rm H})] = -1$ to 6).

TABLE 2
OBJECTS WITH HET+MCDONALD 2.7 METER SPECTROSCOPY

No.	Object	DDO	u	g	r	i	z	σ_{DDO}	σ_u	σ_g	σ_r	σ_i	σ_z
1	SDSS J114149.41−001140.4	19.67	20.49	19.77	19.14	18.05	17.32	0.01	0.05	0.02	0.02	0.02	0.02
2	SDSS J120650.72−010519.1	20.29	22.44	20.81	19.44	17.87	17.11	0.02	0.43	0.06	0.05	0.02	0.03
3	SDSS J120651.91−010435.2	19.31	21.30	19.38	18.59	18.32	18.14	0.01	0.16	0.01	0.02	0.02	0.03
4	SDSS J120709.16−011247.2	16.84	18.12	16.90	16.34	15.70	15.33	0.02	0.01	0.01	0.02	0.01	0.02
5	SDSS J120741.55−010630.9	19.89	22.70	20.07	19.62	18.39	18.17	0.02	1.17	0.15	0.19	0.08	0.09
6	SDSS J123202.54−010232.1	20.33	22.88	20.59	19.25	17.94	17.25	0.04	0.98	0.03	0.02	0.01	0.01
7	SDSS J123208.81−010230.5	20.69	22.52	20.68	19.82	19.37	19.03	0.04	0.31	0.03	0.02	0.02	0.04
8	SDSS J131833.56−004448.4	16.59	18.76	16.80	16.11	15.68	15.41	0.01	0.02	0.02	0.01	0.02	0.01
9	SDSS J143044.16−002853.1	16.99	18.74	17.09	16.53	16.35	16.63	0.01	0.03	0.01	0.01	0.02	0.02

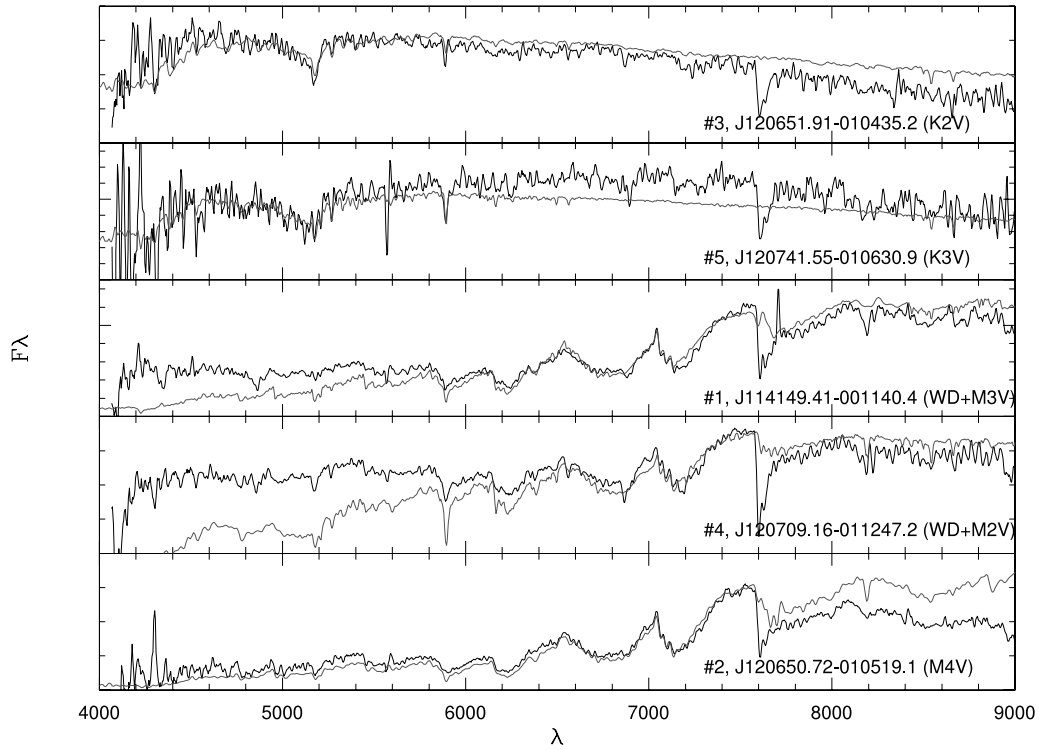

FIG. 3*a*

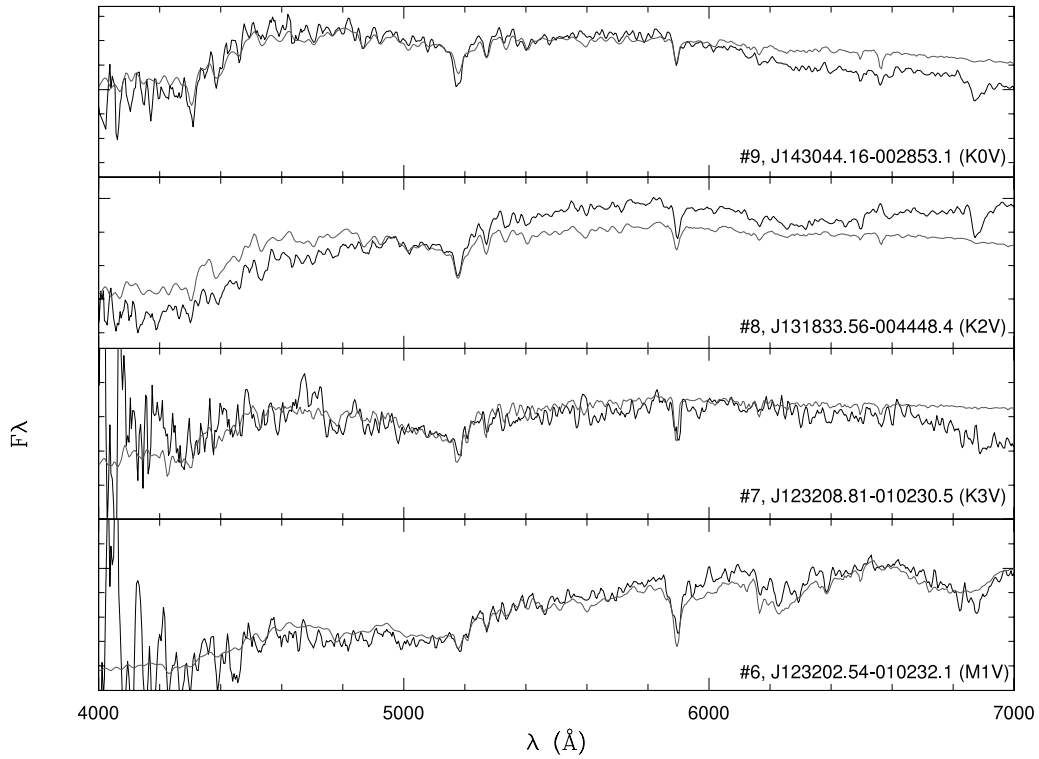

FIG. 3*b*

FIG. 3.—Optical spectra for the white dwarf candidates observed at the HET (*a*) and the 2.7 m (*b*). The light lines indicate the template spectra Pickles (1998) used to classify these objects. Object numbers, coordinates, and spectral types are shown in the bottom right corner. Note that the feature at 7600 Å is telluric and the emission features in object 1 at ∼7700 Å and in object 2 at ∼4300 Å are due to cosmic-ray hits.

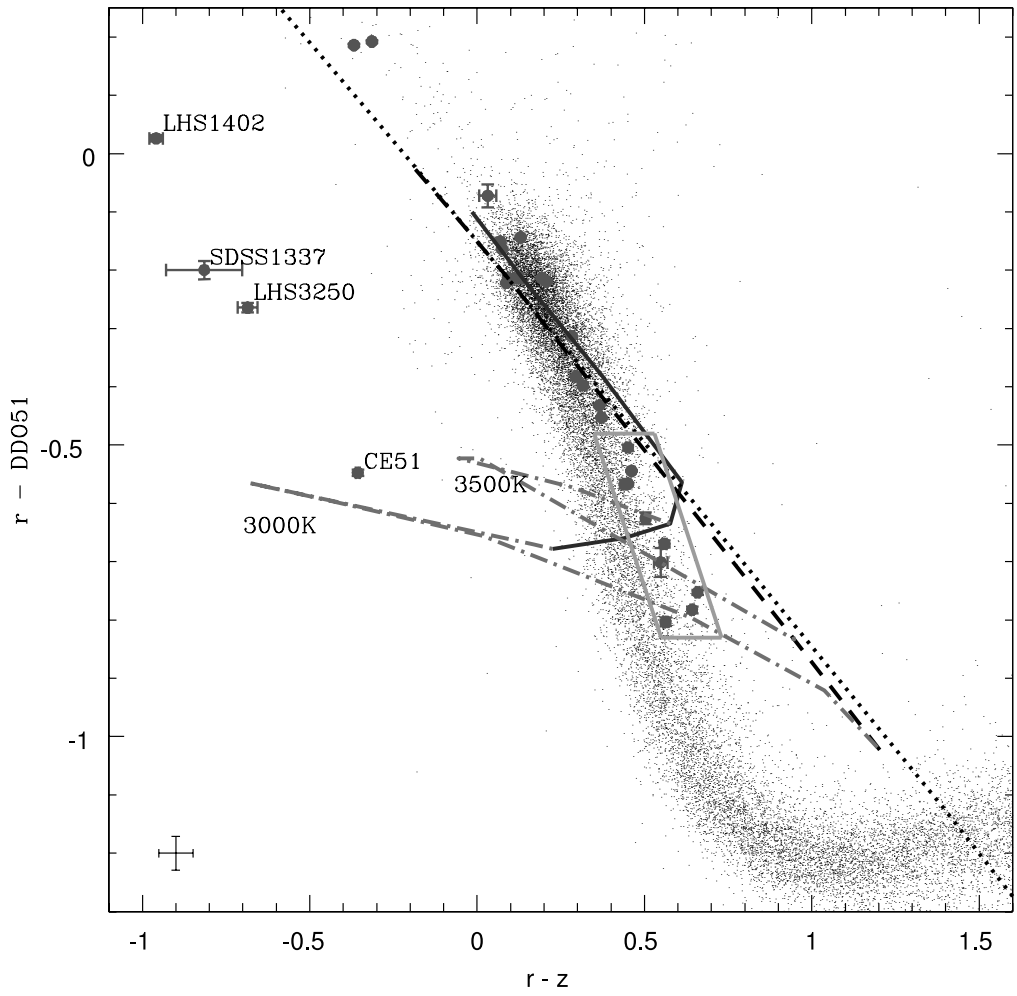

FIG. 4.—An r – DDO51 vs. $r - z$ color-color diagram for 30 known white dwarfs (*filled circles*) and the surrounding field stars (*black dots*). A typical error bar for the field stars is shown in the bottom left corner. Our synthetic photometry of pure H and pure He white dwarf models with 7000 K $\gtrsim T_{\rm eff} \gtrsim$ 3000 K are shown as solid and dashed lines, respectively. Dashed-dotted lines represent mixed atmospheres for 3500 and 3000 K white dwarfs with different compositions, and a blackbody is also shown as a dotted line. The box marks a possible search region for cool white dwarfs.

Temperatures and colors for the observed white dwarfs are given in Table 3. The observed white dwarf sequence is in agreement with our follow-up spectroscopy, and both demonstrate that white dwarfs are much closer to (and more blended with) the main-sequence stars than previously predicted. Cool white dwarfs occupy a region running from the center of the field-star locus ($r - \mathrm{DDO} = -0.1$, $r - z = 0.05$) for $T_{\rm eff} \sim 7000$ K to the red edge of the field-star locus ($r - \mathrm{DDO} = -0.75$, $r - z = 0.65$).

4. DISCUSSION

Our observations demonstrate that the narrowband DDO51 filter, centered on the Mg band, is not as effective at separating white dwarfs from subdwarfs as we expected. White dwarfs with temperatures between 7000 and 5000 K ($-0.10 \geq r - \mathrm{DDO} \geq -0.45$, $0.05 \leq r - z \leq 0.35$) are photometrically indistinguishable from observed field stars. Using template spectra from the Pickles (1998) library, we have measured the equivalent width of the Mg/MgH feature in main-sequence stars. Mg absorption becomes strong enough to affect the photometry in K0 ($T_{\rm eff} \sim 5000$ K) and later-type stars (see Fig. 5). Because of the spread in colors and weak Mg absorption in the F–G type stars, white dwarfs with 7000 K $\geq T_{\rm eff} \geq$ 5000 K have similar colors to F–G stars.

White dwarfs with temperatures in the range 5000–3500 K ($-0.45 \geq r - \mathrm{DDO} \geq -0.80$, $0.35 \leq r - z \leq 0.65$) lie just above the edge of the observed field-star sequence. Until recently, cool white dwarfs were thought to have spectral energy distributions similar to blackbodies. In fact, this is why Claver (1995) suggested that a narrowband filter centered on the MgH feature would place cool white dwarfs above the observed field-star sequence, in which case the DDO51 filter would separate blackbodies from subdwarfs (see Figs. 1 and 4). Although subdwarfs have strong MgH absorption in this temperature range (Fig. 5) and they deviate from blackbodies, observed white dwarfs deviate from blackbodies as well. The effects of collision-induced absorption (CIA) due to molecular hydrogen are expected to be significant below 5000 K (Hansen 1998; Saumon & Jacobson 1999). Figure 4 shows that in these colors, there are no pure H white dwarfs with $T_{\rm eff} \leq 5000$ K and the observed white dwarf sequence actually continues along between the pure H and the pure He models. This is also seen in the $B - V$ versus $V - K$ color-color diagrams of Bergeron et al. (1997, 2001), which implies that either all cool white dwarfs have mixed H/He composition, that the calculated CIA opacities are incorrect, or that there are other neglected physical effects. We note that Bergeron & Leggett (2002) found that all white dwarfs cooler than 4000 K

TABLE 3
DDO51 Photometry for Previously Identified White Dwarfs

Object	R	$r-z$	σ_{r-z}	$r-$ DDO	$\sigma_{r-\mathrm{DDO}}$	T_{eff} (K)	Notes
WD 2323+157	15.04	−0.31	0.01	0.19	0.01	10,170	1
LTT 9491	14.07	−0.37	0.01	0.19	0.01	...	2
CE 157	15.64	0.03	0.03	−0.07	0.02	7000	3
WD 1325+581	16.42	0.07	0.01	−0.15	0.01	6810	4
WD 1633+572	14.68	0.08	0.01	−0.16	0.01	6180	4
WD 2107−216	16.45	0.09	0.01	−0.21	0.01	5830	4
WD 2347+292	15.41	0.13	0.01	−0.14	0.01	5810	4
WD 0752−676	13.58	0.09	0.01	−0.22	0.01	5730	4
CE 162	16.69	0.12	0.01	−0.21	0.01	5730	3
WD 1257+037	15.46	0.21	0.01	−0.22	0.01	5590	4
WD 2248+293	15.14	0.19	0.01	−0.21	0.01	5580	4
WD 0121+401	16.67	0.28	0.01	−0.31	0.01	5340	4
WD 1334+039	14.12	0.36	0.01	−0.43	0.01	5030	4
WD 2002−110	16.36	0.29	0.01	−0.38	0.01	4800	4
WD 0045−061	17.70	0.32	0.01	−0.40	0.01	...	5
WD 1820+609	15.15	0.37	0.01	−0.45	0.01	4780	4
LHS 542	17.53	0.44	0.04	−0.57	0.01	4720	4
WD 1108+207	17.17	0.45	0.01	−0.50	0.01	4650	4
WD 1345+238	15.12	0.45	0.01	−0.57	0.01	4590	4
WD 2251−070	15.10	0.46	0.01	−0.54	0.01	4580	4
CE 40	18.82	0.50	0.01	−0.63	0.01	4580	3
CE 142	18.59	0.55	0.02	−0.70	0.02	4390	3
CE 16	17.59	0.64	0.01	−0.78	0.01	4330	3
WD 1300+263	18.09	0.56	0.01	−0.67	0.01	4320	4
WD 1247+550	17.03	0.66	0.01	−0.75	0.01	4050	4
F351−50	18.37	0.56	0.01	−0.80	0.01	3500:	5
CE 51	17.50	−0.36	0.01	−0.55	0.01	2730:	3
LHS 3250	17.87	−0.69	0.03	−0.26	0.01	...	6
SDSS J133739.40+000142.8	19.16	−0.82	0.11	−0.20	0.02	...	6
LHS 1402	17.86	−0.96	0.02	0.03	0.01	...	5

Notes.—(1) R magnitude and T_{eff} from Bergeron et al. (1997); (2) spectral type DBQA5 (Wesemeal et al. 1993); (3) R magnitude and T_{eff} from Ruiz & Bergeron (2001); (4) R magnitude and T_{eff} from Bergeron et al. 2001; (5) $R_{59\mathrm{F}}$ magnitude and/or T_{eff} from Oppenheimer et al. (2001); (6) SDSS r magnitude.

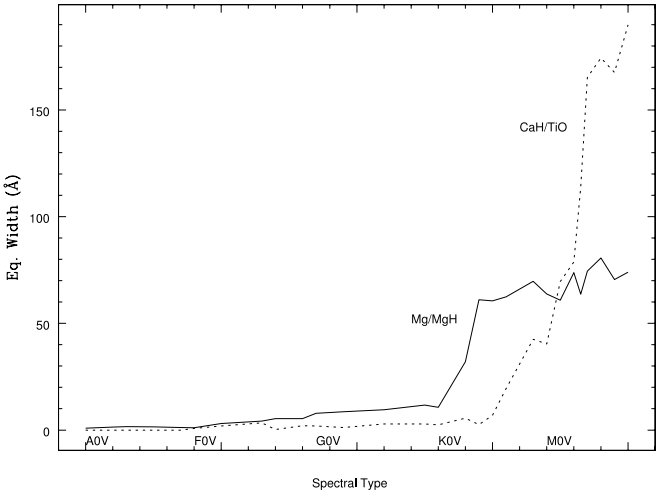

Fig. 5.—Equivalent width of the Mg/MgH and CaH+TiO features measured from Pickles (1998) template spectra. The Mg/MgH feature becomes strong enough to affect the photometry in K0 and later type stars, whereas the CaH+TiO feature dominates at ∼6850 Å for M0 and later type stars.

have mixed H/He atmospheres. Even if the white dwarf model atmospheres and the CIA opacities are right, the question of why we still have not found a pure H white dwarf that shows CIA remains to be answered. A possible explanation for the lack of discovery of such objects may simply be the finite age of the Galactic disk; pure H white dwarfs have not yet cooled enough to show strong CIA absorption.

The effective temperature range between 5000 and 3500 K is the most important regime for white dwarf luminosity function studies since it defines the turnoff of the white dwarf luminosity function and hence the age of the observed population. A single-slit spectrograph would not be efficient in finding those objects preselected by the DDO51 photometry technique, but a wide-field multiobject spectrograph, e.g., Hectospec (Fabricant et al. 1994) with 300 fibers on the converted Multiple Mirror Telescope, might be used productively to carve out regions from the $r-$DDO51 versus $r-z$ color-color diagram to find cool white dwarfs in this range. Figure 4 shows a possible search box for cool white dwarfs. For a 1 deg^2 field at a Galactic latitude $l = 38$, the box includes 234 stars down to $r = 21.5$. Using the Liebert et al. (1988) white dwarf luminosity function and a disk scale height of 250 pc, we expect to find one cool white dwarf per square degree in the search box (5000 K $\geq T_{\mathrm{eff}} \geq$ 3500 K). In other words, the average pointing with the MMT+Hectospec should yield a cool white dwarf. The above field has 660 stars in the color range $-0.80 \leq r-\mathrm{DDO} \leq -0.45$ and 1014 stars

in the range $0.35 \geq r - z \geq 0.65$. Even though the DDO51 filter technique is not as efficient as expected, it rejects at least 65% of main-sequence stars in this temperature range. Therefore, it is $\sim$3 times more efficient than purely spectroscopic (i.e., no prior photometry) surveys. The DDO51 filter is widely used to identify halo stars and to distinguish between giants and dwarfs (Morrison et al. 2000). Thus, DDO51 photometry from the Spaghetti Survey and similar surveys can be used as a by-product to identify cool white dwarf candidates for follow-up spectroscopy.

Four ultracool white dwarfs (CE51, LHS3250, SDSS J133739.40+000142, and LHS1402) lie to the left of the field stars and are clearly separated from the observed sequence of stars because of their depressed near-infrared colors, which are thought to be the result of CIA absorption. DDO51 filter photometry is not necessary for finding ultracool white dwarfs, since these stars have broad molecular features and they can be found using broadband photometry, e.g., in the SDSS. On the other hand, it can help identify the elusive He-rich ultracool white dwarfs because they approximate a blackbody spectral energy distribution. The four ultracool white dwarfs in Figure 4 appear to form a sequence. Ruiz & Bergeron (2001) find an H-dominated atmosphere solution with a temperature estimate of 2730 K for CE51, although infrared photometry is needed to determine the temperature of this star reliably. Simply based on Figure 4, CE51 is more readily explained as a $\sim$3200 K white dwarf of mixed composition. Bergeron & Leggett (2002) tried to fit the spectra for LHS3250 and SDSS J133739.40+000142 and found that they are inconsistent with being pure H atmosphere stars. Mixed H/He atmosphere composition is predicted by Bergeron & Leggett (2002), yet the overall shape of the spectra cannot be fitted with the current model atmospheres. Farihi (2004) has found yet another cool white dwarf, GD392B, consistent with a mixed H/He atmosphere. Estimated tangential velocities for the four ultracool white dwarfs and GD392B are consistent with them being disk objects, and their excess luminosity may be explained if they are low-mass white dwarfs or unusual spectroscopic binaries (Ruiz & Bergeron 2001; Harris et al. 2001; Bergeron 2003; Farihi 2004).

Mixed-atmosphere white dwarfs cool faster than their pure H counterparts, and they are therefore not the defining stars for the age estimates for the Galactic disk, unless no pure H atmosphere white dwarfs exist below 4000 K. Although the four ultracool white dwarfs appear to form a sequence in the $r -$ DDO51 versus $r - z$ color-color diagram, we do not understand their nature at this time. Also, they are not on the theoretically predicted blue hook for cool hydrogen-rich white dwarfs. Our observations demonstrate that optical colors should not be used to estimate the temperatures and ages of ultracool white dwarfs, since current model atmospheres are not fully capable of explaining their observed colors.

Mg/MgH and CaH+TiO are the most prominent features in the optical spectra of subdwarf stars. In addition to the DDO51 filter, we have also investigated the use of an intermediate-band filter centered on the CaH+TiO band at $\sim$6850 Å (Claver 1995) to test whether it can be used to identify white dwarfs. Equivalent width measurements of this band using the Pickles (1998) template spectra are shown in Figure 5. CaH+TiO absorption becomes strong in M0 and later type stars. White dwarfs in this temperature range show depressed infrared colors due to CIA if they have pure H or mixed H/He atmospheres, and they can be identified by using the DDO51 filter if they have pure He atmospheres (true blackbody). The CIA exhibited by ultracool white dwarfs is extremely broadband and monotonically varies throughout the red-infrared region, whereas the CaH/TiO band is very narrowly confined in wavelength. Thus, the CaH+TiO filter, if ratioed with another nearby pseudocontinuum filter, could show a much stronger dependency on temperature and metallicity in main-sequence and subdwarf stars than it does in ultracool white dwarfs. Therefore, the CaH+TiO filter and/or *JHK* infrared photometry may be useful for the identification of cool hydrogen-rich or mixed atmosphere white dwarfs, although broadband photometry surveys are also successful in finding ultracool white dwarfs (e.g., SDSS; Harris et al. 2001; Gates et al. 2004).

We thank Jennifer Claver for useful discussions on reducing MOSAIC data and the NOAO Deep Wide-Field Survey Team for making their reduction procedures available online. We also thank Didier Saumon for making his cool white dwarf model atmospheres available to us and for careful reading of this manuscript. We are grateful to Ed Olsewzki for making his DDO51 photometry data available to us. This material is based on work supported by the National Science Foundation under grant 0307315. The Hobby-Eberly Telescope (HET) is a joint project of the University of Texas at Austin, Pennsylvania State University, Stanford University, Ludwig-Maximilians-Universität München, and Georg-August-Universität Göttingen. The HET is named in honor of its principal benefactors, William P. Hobby and Robert E. Eberly. The Marcario Low Resolution Spectrograph is named for Mike Marcario of High Lonesome Optics, who fabricated several optics for the instrument but died before its completion. The LRS is a joint project of the Hobby-Eberly Telescope partnership and the Instituto de Astronomía de la Universidad Nacional Autonóma de México.

REFERENCES

Bergeron, P. 2003, ApJ, 586, 201
Bergeron, P., & Leggett, S. K. 2002, ApJ, 580, 1070
Bergeron, P., Leggett, S. K., & Ruiz, M. T. 2001, ApJS, 133, 413
Bergeron, P., Ruiz, M. T., & Leggett, S. K. 1997, ApJS, 108, 339
Bertin, E., & Arnouts, S. 1996, A&AS, 117, 393
Claver, C. F. 1995, Ph.D. thesis, Univ. Texas
Fabricant, D. G., Hertz, E. H., & Szentgyorgyi, A. H. 1994, Proc. SPIE, 2198, 251
Farihi, J. 2004, ApJ, 610, 1013
Gates, E., et al. 2004, ApJL, submitted (astro-ph/0405566)
Hansen, B. M. S. 1998, Nature, 394, 860
Harris, H. C., et al. 2001, ApJ, 549, L109
Kilic, M., Winget, D. E., von Hippel, T., & Claver, C. F. 2003, in The XIII European Workshop on White Dwarfs, ed. D. de Martino, R. Silvotti, J.-E. Solheim, & R. Kalytis (Dordrecht: Kluwer), 389
Kleinman, S. J., et al. 2004, ApJ, 607, 426
Knox, R. A., Hawkins, M. R. S., & Hambly, N. C. 1999, MNRAS, 306, 736
Liebert, J. 1979, in IAU Colloq. 53, White Dwarfs and Variable Degenerate Stars, ed. H. M. Van Horn & V. Weidemann (Rochester: Univ. Rochester), 146
Liebert, J., Dahn, C. C., & Monet, D. G. 1988, ApJ, 332, 891
Luyten, W. J. 1979, LHS Catalogue. A Catalogue of Stars with Proper Motions Exceeding 0″.5 Annually (Minneapolis: Univ. Minnesota)
Monet, D. B. A., et al. 1998, VizieR Online Data Catalog, 1252
Montgomery, M. H., Klumpe, E. W, Winget, D. E., & Wood, M. A. 1999, ApJ, 525, 482
Morrison, H. L., et al. 2000, AJ, 119, 2254
Oppenheimer, B. R., Hambly, N. C., Digby, A. P., Hodgkin, S. T., & Saumon, D. 2001, Science, 292, 698
Oswalt, T. D., Smith, J. A., Wood, M. A., & Hintzen, P. M. 1996, Nature, 382, 692

Pickles, A. J. 1998, PASP, 110, 863
Ruiz, M. T., & Bergeron, P. 2001, ApJ, 558, 761
Salaris, M., García-Berro, E., Hernanz, M., Isern, J., & Saumon, D. 2000, ApJ, 544, 1036
Saumon, D., & Jacobson, S. B. 1999, ApJ, 511, L107
Wesemael, F., et al. 1993, PASP, 105, 761
Winget, D. E., Hansen, C. J., Liebert, J., Van Horn, H. M., Fontaine, G., Nather, R. E., Kepler, S. O., & Lamb, D. Q. 1987, ApJ, 315, L77
Wood, M. A., & Oswalt, T. D. 1998, ApJ, 497, 870